Separation Science and Technology
Publication details, including instructions for authors and subscription information:
http://www.informaworld.com/smpp/title~content=t713708471

Gravity Filtration with Accretion of Slurry at Constant Rate

D. E. Smiles[a]; J. H. Knight[b]; T. X. T. Nguyen-hoan[c]
[a] DIVISION OF ENVIRONMENTAL MECHANICS, CANBERRA CITY, A.C.T., AUSTRALIA [b] DIVISION OF MATHEMATICS AND STATISTICS, CANBERRA CITY, A.C.T., AUSTRALIA [c] DIVISION OF ENVIRONMENTAL MECHANICS CSIRO, CANBERRA CITY, A.C.T., AUSTRALIA

To cite this Article Smiles, D. E. , Knight, J. H. and Nguyen-hoan, T. X. T.(1979) 'Gravity Filtration with Accretion of Slurry at Constant Rate', Separation Science and Technology, 14: 3, 175 — 192
To link to this Article: DOI: 10.1080/01496397908066957
URL: http://dx.doi.org/10.1080/01496397908066957

SEPARATION SCIENCE AND TECHNOLOGY, 14(3), pp. 175–192, 1979

Gravity Filtration with Accretion of Slurry at Constant Rate

D. E. SMILES

DIVISION OF ENVIRONMENTAL MECHANICS

J. H. KNIGHT

DIVISION OF MATHEMATICS AND STATISTICS

T. X. T. NGUYEN-HOAN

DIVISION OF ENVIRONMENTAL MECHANICS
CSIRO
CANBERRA CITY, A.C.T. 2601, AUSTRALIA

Abstract

The separation of liquid from solid in many industrial effluents may be described by a physical theory developed originally to describe one-dimensional movement of water in a swelling soil. The theory makes use of *measured* hydraulic conductivity–liquid content, and liquid content–liquid potential relations. Both these functions have been found to be well defined, as required for their use in the theory.

The process of gravity filtration is explored in terms of this theory for vertical columns of effluent, to the top of which additional effluent is applied continuously at a constant rate, and from the bottom of which the liquid phase escapes through a membrane which prevents escape of the solid phase. The physics of the process is discussed, and illustrative calculations and experimental data are presented for one aspect of the process for which a quasi-analytical solution is possible. The calculations are simplified using the flux–concentration relation of Philip.

The approach permits reliable calculation of the liquid–solid profile and the filtration rate for the process.

INTRODUCTION

If one assumes that the solid particles in a solid–liquid suspension do not interact, and that they settle to an incompressible cake during filtration, then the separation processes of filtration and sedimentation appear well understood.

For many colloidal systems, however, particle–particle "interaction" occurs at quite high liquid contents and the separation process involves significant conceptual problems in filtration as well as sedimentation.

Smiles (*1*, *2*) has presented a theory that permits prediction of the important aspects of constant pressure and constant rate filtration of materials in which the hydraulic conductivity–liquid content, $K(\vartheta)$, and liquid potential–liquid content, $\Psi(\vartheta)$, relations are well-defined. ϑ is the volume of liquid per unit volume of solid. This approach has been tested with bentonite particles (*2*) and with red-mud produced as an effluent by the aluminum industry (*3*).

In many situations, however, the volume of effluent produced is so great that mechanical filtration procedures are impracticable and separation can only be effected by gravity. Smiles (*4*) discussed the energetics of sedimentation and self-weight filtration of such slurries and showed that drainage enhances the liquid recovery. The effects were demonstrated in terms of equilibrium profiles. In this paper we examine the process of gravity (or self-weight) filtration for a particulate slurry with well defined $K(\vartheta)$ and $\Psi(\vartheta)$ relations. In particular, we concern ourselves with the case of an initially uniform vertical column of effluent of length Z to which further slurry is added at a constant rate R. Liquid, but not solid, escapes from the bottom through a filter membrane at a rate $V_0(t)$ which is a function of time t.

THEORY

In a porous material in which $K(\vartheta)$ and $\Psi(\vartheta)$ are well defined, the one-dimensional volume flux density of liquid relative to solid, V, is related to $\partial\Phi/\partial z$, the space gradient of the total liquid potential, by Darcy's law (*1*, *2*), viz.,

$$V = -K(\vartheta)\frac{\partial \Phi}{\partial z} \tag{1}$$

If we define our potentials as work per unit weight of liquid, then the potential takes convenient dimensions of length (*5*) and the total potential Φ may be written

$$\Phi(z) = \Psi[\vartheta(z)] - z - \int_z^\infty \gamma(z)\,dz + P \tag{2}$$

where z is the vertical coordinate defined positive downward, γ is the wet specific gravity of the slurry, P is the normal stress due to any external load, and our integration from ∞ simply means that we encompass all the suspension above the point z.

The material coordinate, m, defined by

$$dm/dz = (1 + \vartheta)^{-1} \tag{3}$$

then permits us to write the liquid continuity equation in the form

$$\left(\frac{\partial \vartheta}{\partial t}\right)_m = -\left(\frac{\partial V}{\partial m}\right)_t \tag{4}$$

and Eqs. (1)–(4) yield the nonlinear diffusion equation

$$\frac{\partial \vartheta}{\partial t} = \frac{\partial}{\partial m}\left(D'(\vartheta)\frac{\partial \vartheta}{\partial m} - K'(\vartheta)\right) \tag{5}$$

in which $K'(\vartheta) = (\gamma_c - 1)K(\vartheta)(1 + \vartheta)^{-1}$, $D'(\vartheta) = K'(\gamma_c - 1)^{-1}\,d\Psi/d\vartheta$, and γ_c is the particle specific gravity.

Slurry, with an initial uniform liquid content ϑ_n, is discharged at rate R into a vessel at the bottom of which is a membrane permitting free passage of liquid but not solid. We define $m = 0$ and $z = 0$ at this outflow membrane. We note that m is the cumulative volume of solid per unit cross section above $z = 0$.

We take as our initial condition

$$\vartheta = \vartheta_n, \qquad \text{for } 0 < m < M,\ t = 0 \tag{6}$$

where M is the initial material length of the column of slurry of length Z, i.e.,

$$M = (1 + \vartheta_n)^{-1}Z \tag{7}$$

If then the liquid escapes to a pool of free liquid at atmospheric pressure and $z = 0$, then the interparticle stress [or the "solids compressive pressure" (*2*)] in the slurry on the outflow membrane, $-\Psi_0(t)$, at any time t, is equal to the initial value $\Psi_0(0) = \gamma_n Z + P$, plus a component $\gamma_n Rt$ due to the added slurry, minus that due to the cumulative amount of liquid which has drained from the base, i.e.,

$$-\Psi_0(t) = \gamma_n Z + P + \gamma_n R t - \int_0^t V_0(t)\,dt \tag{8}$$

in which γ_n is the initial wet specific gravity of the slurry.

This condition may be simplified to

$$-\frac{d\Psi_0}{dt} = \gamma_n R - V_0(t), \qquad m = 0,\ t > 0 \tag{9}$$

In the experiments described here, the properties of the bentonite used permit two substantial simplifications to the analysis. First, we find that $D'\,\partial\vartheta/\partial m$ is generally much greater than $K'(\vartheta)$: this condition allows us to simplify Eq. (5) by neglecting $K'(\vartheta)$ so that we now seek a solution to the nonlinear diffusion equation

$$\frac{\partial\vartheta}{\partial t} = \frac{\partial}{\partial m}\left[D'(\vartheta)\frac{\partial\vartheta}{\partial m}\right] \tag{10}$$

Physically, this means that even though the driving force for filtration originates in the self-weight of the column (cf. Eq. 8), the flux due to gravity, $K'(\vartheta)$, is insignificant compared with that identified with $\partial\Psi/\partial m$.

Second, we examine the situation where $\gamma_n R \gg V_0(t)$. The boundary condition (9) then becomes

$$-\frac{d\Psi_0}{dt} = -\left(\frac{d\Psi_0}{d\vartheta_0}\frac{d\vartheta_0}{dt}\right) = \gamma_n R, \qquad m = 0,\ t \gg 0 \tag{11}$$

with $\vartheta = \vartheta_0$ at $m = 0$.

We note that as a consequence of the condition that $\gamma_n R \gg V_0(t)$, we infer that at the upper surface of the slurry $\partial\vartheta/\partial m = 0$. Our analysis is therefore based on the notion of a semi-infinite column.

It should be noted that neither assumption prejudices our test of the basic principles involved in the analysis.

Our solution of Eq. (10) subject to conditions (6) and (11) is based on the concept of the flux-concentration relations, $F(\Theta, t)$, of Philip (*6*). In this relation $\Theta = (\vartheta - \vartheta_n)/(\vartheta_0 - \vartheta_n)$ and

$$\begin{aligned} F(\Theta, t) &= V(\vartheta)/V_0 \\ &= \int_{\vartheta_n}^{\vartheta}\left(\frac{\partial m}{\partial t}\right)d\vartheta \Bigg/ \int_{\vartheta_n}^{\vartheta_0(t)}\left(\frac{\partial m}{\partial t}\right)d\vartheta \end{aligned} \tag{12}$$

This equation arises by integrating the continuity equation expressed in the form

$$\left(\frac{\partial m}{\partial t}\right)_{\vartheta} = \left(\frac{\partial V}{\partial \vartheta}\right)_{t} \tag{13}$$

using the condition of semi-infinity which implies that $V(\vartheta_n) = 0$.

As Philip (*6*) points out, both Θ and $F(\Theta, t)$ decrease as m increases, and for any t, $F(\Theta, t)$ is a nondecreasing function of Θ such that $F(1, t) = 1$ and $F(0, t) = 0$. The time dependence of $F(\Theta, t)$ in our problem arises in principle because $\vartheta_0(t)$ decreases with t. As a result, $D'(\vartheta_0)$ changes to produce variation in the "shape" of $F(\Theta, t)$. As we see in Eq. (12), however, $F(\Theta, t)$ is the ratio of integral properties of the process, and variation in the shape of $F(\Theta, t)$ will be much less than the variation in $D'(\vartheta_0)$.

The solution to the problem using this relation of Philip (*6*) is based on the integration of the flux equation (1) and the continuity equation (13).

The diffusional form of Eq. (1) for the case where $V_0 \gg K'(\vartheta_n)$ [and by implication $V_0 \gg K'(\vartheta_n) > K'(\vartheta)$] is

$$V = -D'(\vartheta)\frac{\partial \vartheta}{\partial m} \tag{14}$$

If we substitute $F(\Theta, t)$ in this equation and integrate, we obtain

$$V_0 m = \int_{\vartheta_0(t)}^{\vartheta} D'(\vartheta)/F(\Theta, t)\, d\vartheta \tag{15}$$

Furthermore, if we substitute for m from Eq. (15) in the integrated form of Eq. (13), we obtain

$$\int_0^t V_0(t)\, dt = \int_{\vartheta_n}^{\vartheta_0(t)} m\, d\vartheta \tag{16}$$

which equates the cumulative flux at the boundary to the change in liquid content in the column. Integrating by parts, we then obtain

$$V_0(t) \int_0^t V_0(t)\, dt = -\int_{\vartheta_0(t)}^{\vartheta_n} (\vartheta - \vartheta_n)[D'(\vartheta)/F(\Theta, t)]\, d\vartheta \tag{17}$$

If we define the cumulative outflow $I(t)$ by

$$I(t) = \int_0^t V_0(t)\, dt$$

Eq. (17) takes the more useful form

$$\frac{1}{2}\frac{dI^2}{dt} = \int_{\vartheta_n}^{\vartheta_0(t)} (\vartheta - \vartheta_n)[D'(\vartheta)/F(\Theta, t)]\, d\vartheta \tag{18}$$

Integration of Eq. (18) using Eq. (11) then yields

$$\gamma_n R I^2 = -2\int_{\Psi_0(t=0)}^{\Psi_0(t)} \left(\int_{\vartheta_n}^{\vartheta_0(t)} (\vartheta - \vartheta_n)[D'(\vartheta)/F(\Theta, t)]\, d\vartheta\right) d\Psi \tag{19}$$

Were $F(\Theta, t)$ known precisely, then the set of Eqs. (11), (15), and (19) would permit calculation of all aspects of the dewatering process. Unfortunately, $F(\Theta, t)$ is not, in general, known *a priori*; as we demonstrate below, however, it is sufficiently robust a function that we may often guess a form which permits predictive use of Eqs. (15) and (19) with acceptable errors.

In our experiments we test that data are consistent with Eqs. (15) and (19) by graphing $\vartheta(V_0 m)$ and $\gamma_n R I^2$ $[\gamma_n R t = \Psi(t)]$ for a series of experiments in which R is varied. This consistency confirms that the diffusion model (Eq. 10) is valid and that the assumptions concerning the initial and boundary conditions are justified.

In addition, we investigate the predictive role of Eqs. (15) and (19) by calculating $\vartheta(V_0 m)$ and $\gamma_n R I^2$ $(\gamma_n R t)$ using $D'(\vartheta)$ and $\Psi(\vartheta)$ data (obtained independently) together with a physically based estimate of $F(\Theta, t)$.

Estimation of $F(\Theta, t)$

For the case of constant pressure filtration there exists (*7*) a rapidly converging iterative procedure for accurate calculation of $F(\Theta)$ [note that since ϑ_0 is constant in this case, there is no t-dependence in $F(\Theta, t)$]. No such scheme appears to exist for constant rate filtration (*2*) or for the problem discussed here. Any method for estimating the correct $F(\Theta, t)$ relation must therefore be justified experimentally for each particular situation.

In our case the choice of $F(\Theta, t)$ depends on comparison between constant-pressure and constant-rate filtration: in the former process Ψ_0 and ϑ_0 are constant and V_0 decreases as $t^{-1/2}$ (*1*); in the latter process, V_0 is constant, $|d\Psi_0/dt|$ increases with t, and ϑ_0 decreases. Experimentally, however, we find that the same $F(\Theta)$ relation may be used to calculate profiles and filtration rates for both processes. In addition, the possibility that $F(\Theta, t)$ is time-dependent in the latter process appears not to be important, and from here on we write $F(\Theta)$.

Now for our specific case $d\Psi_0/dt$ is constant, so our process is in a sense intermediate between the behavior of these other two. We therefore assume (at least for bentonite and the conditions of our experiments) that we may use, without significant error, the $F(\Theta)$ relation strictly appropriate to the case of constant pressure filtration. As a result we can use the appropriate analog of the Philip and Knight (*7*) iterative procedure to determine a sufficiently good approximation to the correct $F(\Theta)$.

Iterative Solution of Eq. (1)

As we point out above, the scheme is analogous to that of Philip and Knight (*7*) for the constant concentration boundary condition. The convergence of the scheme is discussed in that paper.

Briefly, we choose a physically realistic $F(\Theta)$ function, $F_1(\Theta)$, and using $D'(\vartheta)$ we calculate $\vartheta_1(V_0m)$ from Eq. (15). This profile yields a second estimate of $F(\Theta)$, $F_2(\Theta)$, using the equation

$$F_2(\Theta) = \int_{\vartheta_n}^{\vartheta} (V_0m)\, d\vartheta \Big/ \int_{\vartheta_n}^{\vartheta_0} (V_0m)\, d\vartheta \tag{20}$$

$F_2(\Theta)$ is then used to calculate $\vartheta_2(V_0m)$. The process is repeated until successive estimates of $F(\Theta)$ differ by some arbitrarily small amount.

EXPERIMENTAL

"Western bentonite" supplied by the National Lead Co., Houston, Texas was used in all experiments. The clay was mixed with an appropriate weight of distilled water in approximately 4 liter volumes, and aliquots were taken as required.

Determination of $D'(\vartheta)$

The method described in Refs. *8* and *9* based on that of Matano (*10*) was used to determine $D'(\vartheta)$. A vertical column of clay was subjected to a constant pressure of 14.55 m of water, and water was permitted to escape through a 0.45-μm membrane at its base to atmospheric pressure. At a particular elapsed time the pressure was released, the column was cut into short sections, and the liquid content of each was determined by oven drying at 105°C. The experiment was repeated at the same pressure for five different elapsed times. The results were plotted as $\vartheta(\lambda)$, where $\lambda = mt^{-1/2}$. $D'(\vartheta)$ was calculated using the equation

$$D'(\vartheta) = -(d\lambda/d\vartheta) \int_{\vartheta_n}^{\vartheta} (\lambda/2)\, d\vartheta \tag{21}$$

Figure 1 shows $\vartheta(\lambda)$ for these experiments, Fig. 2 shows the corresponding derived $F(\Theta)$ curve, and Fig. 3 shows the derived $D'(\vartheta)$ data.

Determination of $\Psi(\vartheta)$

The $\Psi(\vartheta)$ relation for this sample of bentonite, shown in Fig. 4, was determined using the method described in Ref. *4*.

Filtration Experiments

The experiments were designed to realize conditions (6) and (11).

A uniform column of clay was placed in a sectioned stainless steel cylinder, 3.82×10^{-2} m internal diameter, mounted on a screen supporting a 0.45-μm Gelman membrane. The membrane permits easy escape of the water to a pool at atmospheric pressure, but prevents the escape of the clay particles. The cumulative outflow, I, was measured using a calibrated capillary tube, the cross-sectional area of which varied by less than $\pm 2\%$.

The clay was loaded hydraulically using mineral oil, the pressure of which was increased by raising a mercury reservoir at a constant rate. The equipment is shown diagrammatically in Fig. 5.

Each experiment was terminated when an imposed pressure $(\gamma_n Rt)$ of 6.1 m water was attained. The column was then sectioned and the liquid content profile determined by oven drying at 105°C.

Table 1 summarizes the salient features of the experimental sequence. All experiments were performed in a room held at 21 ± 1 °C, and care was taken to minimize evaporation from the column during the experiment and during sectioning.

Figure 6(a) shows $\vartheta(V_0 m)$ obtained from these experiments, while Fig. 7 shows the cumulative outflow I in the form $(\gamma_n R)^{1/2} I$ vs $\gamma_n Rt$ for each experiment.

DISCUSSION

Determination of $D'(\vartheta)$

The data from the five constant pressure filtration experiments shown in Fig. 1 reveal that $\vartheta(\lambda)$ is unique despite the different times of sampling. We conclude that the process can be examined in terms of the diffusion model represented by Eq. (10). By implication, both $\Psi(\vartheta)$ and $D'(\vartheta)$ are well defined; we therefore proceed to use these data to calculate

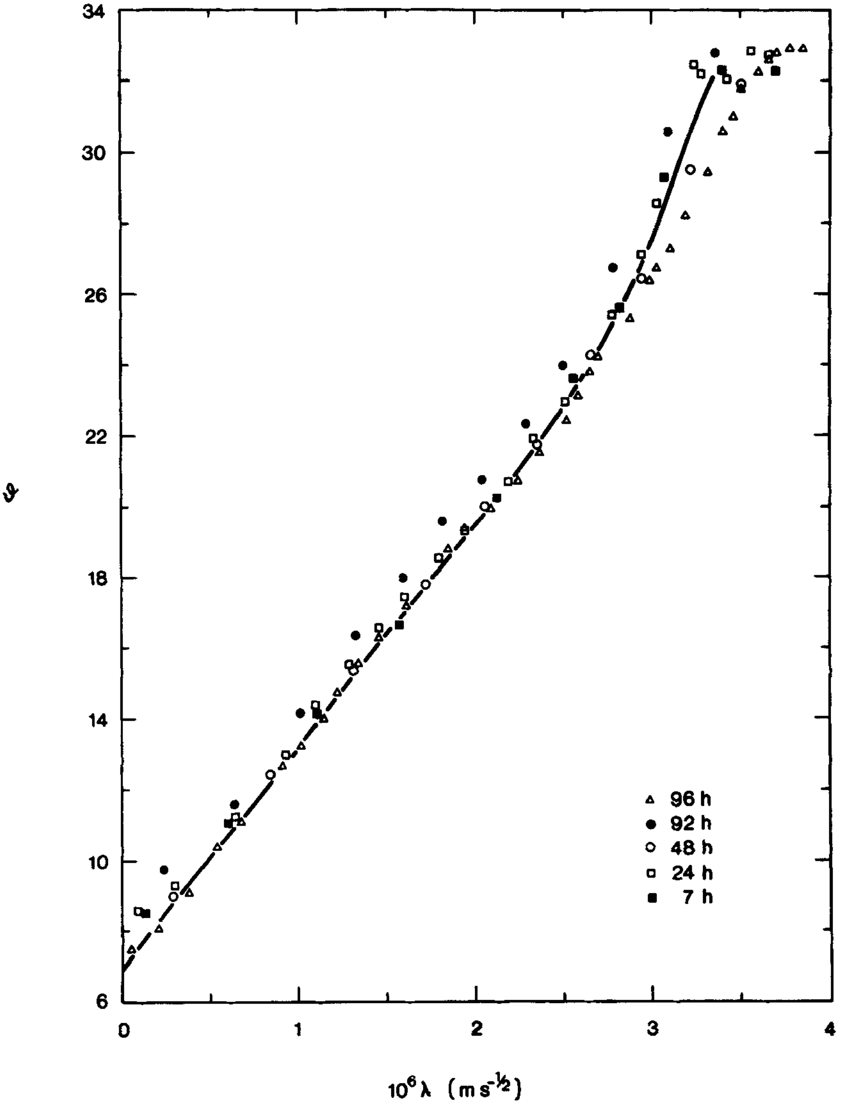

FIG. 1. Liquid content, ϑ, vs reduced space, $\lambda = mt^{-1/2}$, for five filtration experiments in which a constant pressure of 14.55 m of water was imposed. The experiments were terminated at the times (in hours, h) shown in the figure. The smooth curve was calculated using Fig. 3 and $F = \Theta(2 - \Theta)$ as explained in the text.

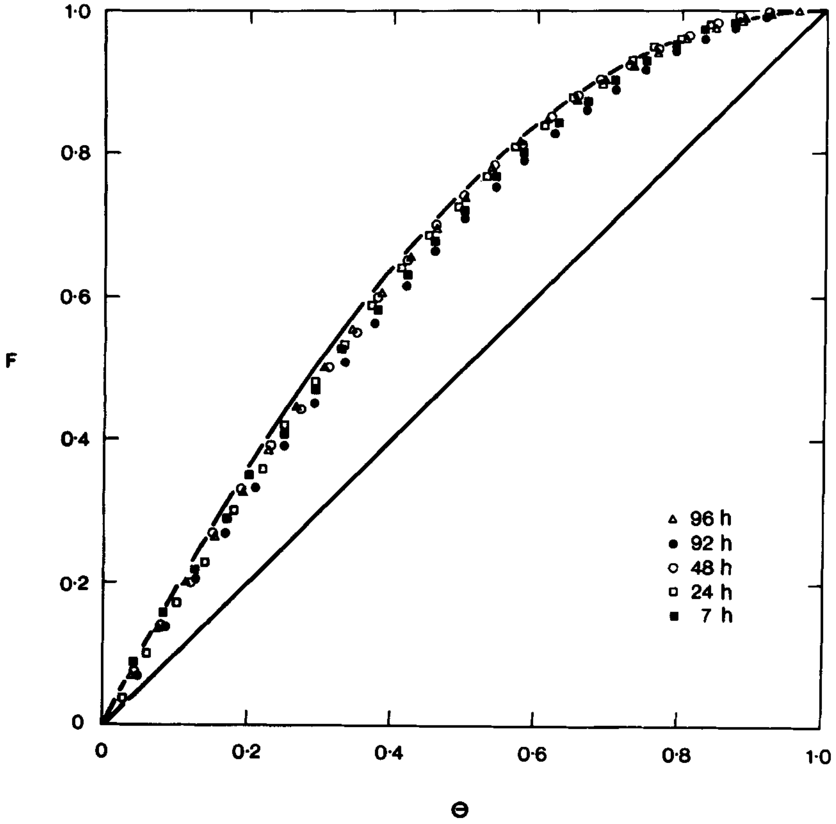

FIG. 2. $F(\Theta)$ relations for the five experiments shown in Fig. 1, together with $F = \Theta(2 - \Theta)$. The symbols correspond to those in Fig. 1.

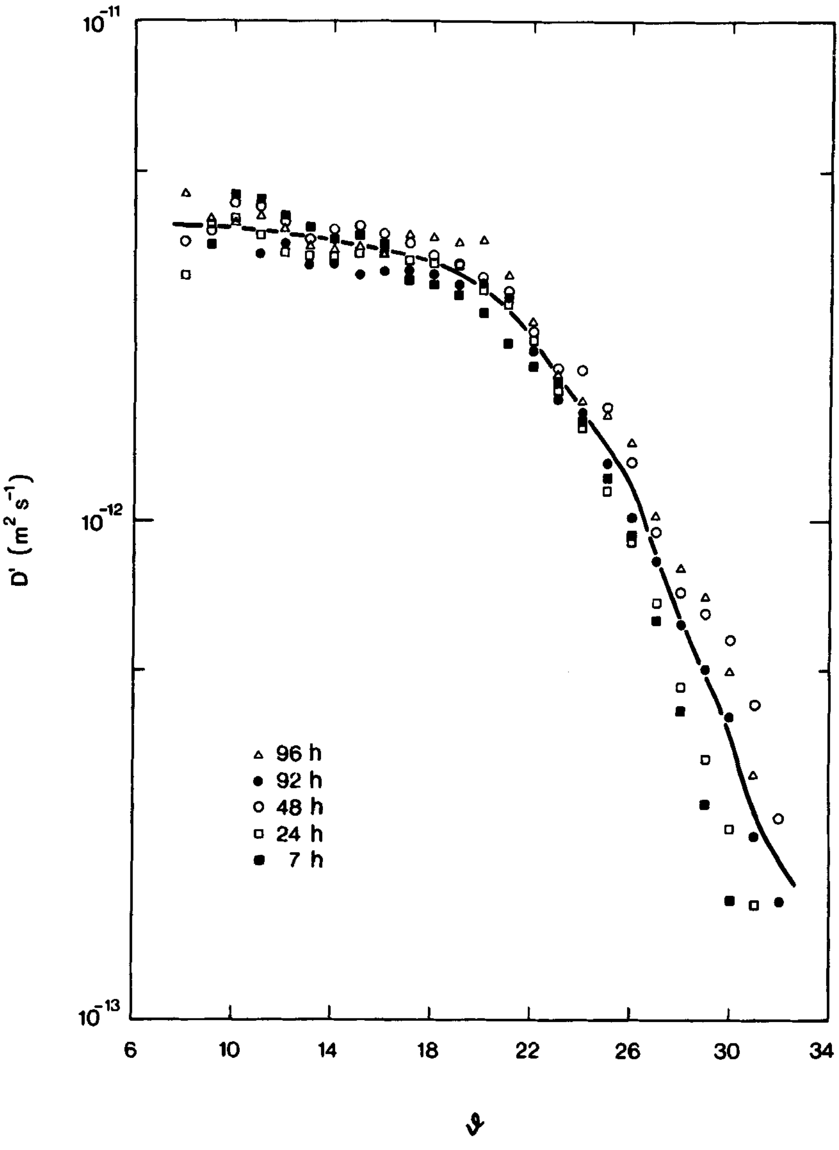

FIG. 3. $D'(\vartheta)$ data derived from smooth curves drawn through the individual experimental data sets of Fig. 1. The dashed line is the arithmetic mean used for predictive calculation.

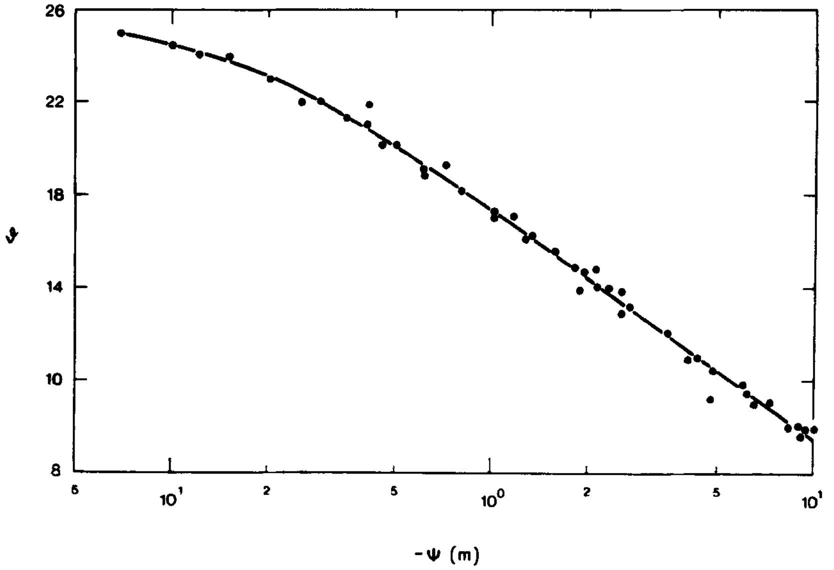

FIG. 4. $\Psi(\vartheta)$ relation for the bentonite used in these experiments.

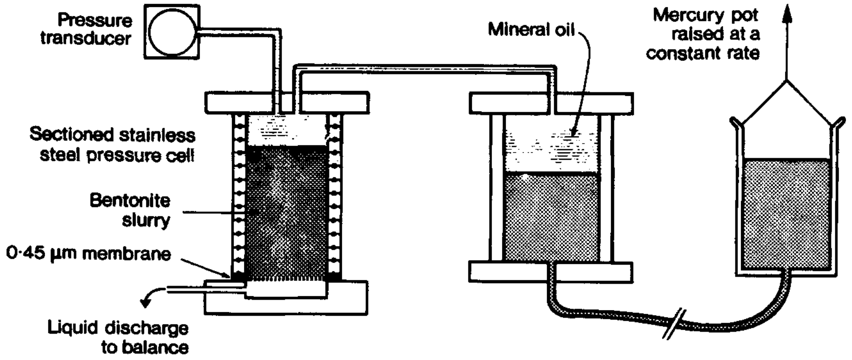

FIG. 5. Diagram of the equipment used to perform constant loading rate experiments.

TABLE 1

Summary of Experimental Conditions Imposed during Constant Loading Rate Experiments

Symbol[a]	Initial liquid content, ϑ_n m³/m³ = 1	Loading rate, $\gamma_n R$ (m/sec)	Sampling time (sec)
○	32.97	5.7×10^{-5}	1.068×10^{5}
●	33.00	5.9×10^{-5}	1.051×10^{5}
△	32.87	9.6×10^{-5}	6.318×10^{4}
▲	32.85	9.6×10^{-5}	6.360×10^{4}
□	32.85	3.4×10^{-4}	1.785×10^{4}
■	32.76	3.4×10^{-4}	1.788×10^{4}
◐	32.89	9.03×10^{-4}	6.780×10^{3}

[a] Corresponds to symbols used on Figs. 6(a) and 7.

$D'(\vartheta)$. It is useful, however, to obtain an estimate of the scatter in both $D'(\vartheta)$ and $F(\Theta)$, so rather than determine these functions for the average of five experiments, we determine them for the smooth curve drawn through each set of data. $D'(\vartheta)$ curves are shown in Fig. 2, and $F(\Theta)$ curves, calculated using the equation (Ref. *6*)

$$F(\Theta) = \int_{\vartheta_n}^{\vartheta} \lambda \, d\vartheta \Big/ \int_{\vartheta_n}^{\vartheta_0} \lambda \, d\vartheta \tag{22}$$

are shown in Fig. 3. Comparison of Figs. 2 and 3 reveals that the scatter in $D'(\vartheta)$ is about ±12% with a maximum at the limits of ϑ of about ±40%, and therefore much greater than the maximum of about ±1.5% in $F(\Theta)$.

This difference is to be expected since $F(\Theta)$ is a ratio of integral properties of the solution while $D'(\vartheta)$ involves the differentiation of experimental data. The observation has the important consequence that, in general, error in the use of Eqs. (15) and (19) will be dominated by the scatter in $D'(\vartheta)$ rather than by the scatter in $F(\Theta)$, and the estimation of $F(\Theta)$ for other processes is by implication less critical.

For example, if we calculate $\vartheta(\lambda)$ using the "average" $D'(\vartheta)$ of Fig. 2 and assert from experience that $F = \Theta(2 - \Theta)$, then we obtain the smooth curve in Fig. 1. The prediction is clearly excellent. Note that $F(\Theta) = \Theta(2 - \Theta)$ is exact for the profile given by

$$\frac{\vartheta_n - \vartheta}{\vartheta_n - \vartheta_0} = \frac{\lambda_n - \lambda}{\lambda_n}$$

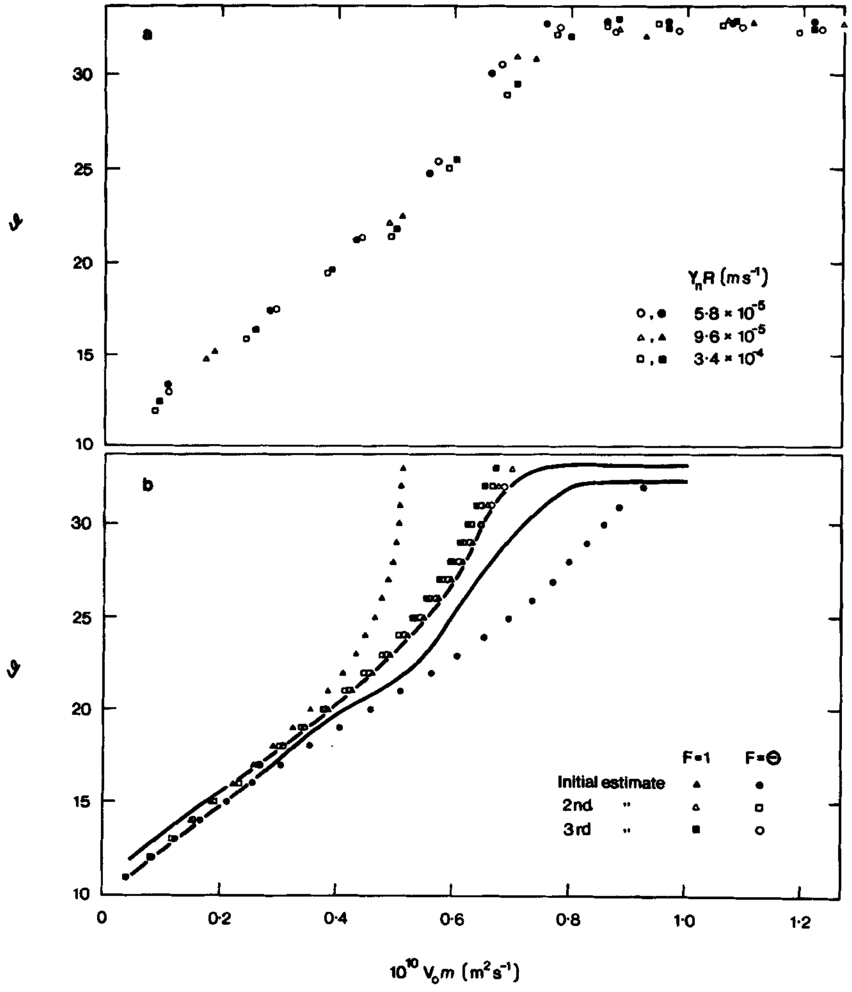

FIG. 6. (a) Liquid content, ϑ, vs reduced space, $V_0 m$, data for Experiments 1–6 identified in Table 1. The loading rates are identified in the figure. (b) $\vartheta(V_0 m)$ data calculated using Fig. 3 and Eq. (15). These data demonstrate the rapidity of convergence of the iterative scheme for the two worst guesses of $F(\Theta)$. The smooth curves present the limits of the experimental data shown in Fig. 6b.

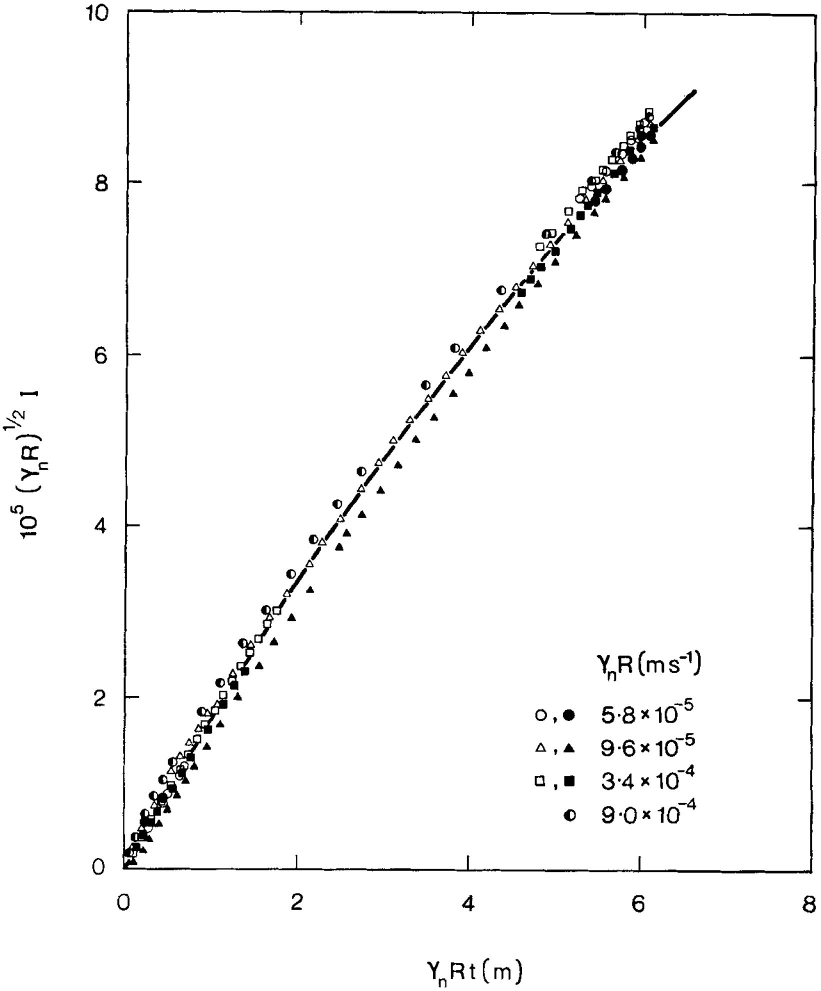

FIG. 7. Reduced cumulative outflow, $(\gamma_n R)^{1/2} I$, vs reduced time, $\gamma_n Rt$, data obtained for the experiments shown in Table 1. The dashed line was predicted using Fig. 3, Fig. 4, Eq. (19), and the "correct" $F(\Theta)$ inferred from Fig. 6b.

Constant Loading Rate Experiments

Referring now to Figs. 6 and 7, we observe that the experimental data are reduced to unique curves as required by Eqs. (15) and (19) despite the great variation of $(\gamma_n R)$ between the experimental sets shown in Table 1. The figures therefore confirm that the assumptions leading to the diffusion equation (10) are valid and that the boundary condition, Eq. (11), is realized.

We now examine our supposition that $F(\Theta)$ appropriate to the constant concentration boundary condition will permit acceptable accuracy in predictive use of Eqs. (15) and (19). In order to demonstrate the iterative procedure in this calculation, we have consciously made the worst possible upper and lower guesses for $F(\Theta)$, viz., $F = 1$ and $F = \Theta$ (see Ref. *6* for more detail). The initial and two subsequent estimates of $\vartheta(V_0 m)$ for each initial $F(\Theta)$ are shown in Fig. 6(b) together with the dashed limits to the experimental data of Fig. 6(a).

The improvement is rapid and the prediction good, considering the scatter in $D'(\vartheta)$. We hasten to reiterate, however, that the $F(\Theta)$ we have discussed in this way is the one appropriate to the constant concentration boundary condition and therefore only an estimate for our experimental conditions. The excellence of the estimation would have to be established for other materials, but as we show, the procedure is direct and relatively simple.

The predictive power of Eq. (19) is demonstrated by the dashed line in Fig. 7. Again we use the $D'(\vartheta)$ and $\Psi(\vartheta)$ data of Figs. 3 and 4, but we use the "ultimate" $F(\Theta)$ relation involved in Fig. 6(b). Again the prediction is excellent.

We conclude that for the materials used in these experiments the approach provides a precise method for predicting the features of this type of filtration.

Dimensional Observations

It is evident that $\gamma_n R$ may be eliminated explicitly from Eqs. (6), (10), and (11) by using the reduced coordinates $T = \gamma_n R t$ and $X = (\gamma_n R)^{1/2} m$. $\vartheta(X, T)$ is thus a universal function describing the evolution of the family of profiles with the same initial liquid content, ϑ_n.

We may therefore immediately infer the evolution of liquid content profiles for any value of $(\gamma_n R)$ $[\gg V_0]$ using experimental data for one particular value of $\gamma_n R$.

Conversion to "Real" Space

The calculation of the liquid content profile is most readily performed, as we show, in Lagrangian space. The recalculation to "physical space" is straightforward since we recall from Eq. (3) that

$$z(m, t) = \int_0^m [1 + \vartheta(m, t)]\, dm$$

The Solution to Eq. (10) Subject to Conditions (6) and (9)

In this case $V_0(t)$ is of the same order of magnitude and perhaps greater than $\gamma_n R$. The situation will arise in bentonite if Z is great compared with Rt. Equation (15) again yields the liquid and solid profiles, but appropriate values of $\vartheta_0(t)$ must be obtained by solving numerically the equation

$$\left(\frac{d\vartheta_0}{dt}\right)\left(\frac{d\Psi_0}{d\vartheta_0}\right) = \gamma_n R - I^{-1}(t) \int_{\vartheta_0(t)}^{\vartheta_n} (\vartheta - \vartheta_n)[D'(\vartheta)/F(\Theta, t)]\, d\vartheta \quad (23)$$

In the particular case where $V_0(t) = \gamma_n R$, we have $d\Psi_0/dt = 0$. In this situation the interparticle stress at $m = 0$ is constant, and the process is one of constant pressure filtration.

In fact, the conductivity $K'(\vartheta)$ of bentonite is so small that even in the extreme situation, where $\gamma_n R = 0$, the process may be treated practically as a constant pressure problem.

The Effect of Hysteresis

Preliminary investigation indicates that for dispersed colloidal suspensions, hysteresis in $\Psi(\vartheta)$ is unimportant (*11*). The analysis fails, however, for those materials for which $\Psi(\vartheta)$ is *not* well defined. In general this situation would arise where $\gamma_n R < \int_0^t V_0(t)\, dt/t$.

CONCLUSION

We conclude that for materials where $\Psi(\vartheta)$ and $K(\vartheta)$ are well defined, various aspects of gravity filtration with a constant accretion rate of slurry may be predicted using a diffusion analysis based on Darcy's law.

SYMBOLS

$K(\vartheta)$	hydraulic conductivity (m/sec)
ϑ	volumetric liquid content per unit volume of solid

ϑ_n	initial volumetric liquid content per unit volume of solid
ϑ_0	volumetric liquid content per unit volume of solid at $x = 0$
$\Psi(\vartheta)$	liquid potential (m liquid)
Z	initial depth of slurry (m)
R	rate of addition of slurry (m/sec)
$V_0(t)$	filtration rate (m/sec)
t	time (sec)
V	volume flux of liquid relative to the solid (m/sec)
Φ	total liquid potential (m liquid)
z	space coordinate (m)
γ	wet specific gravity of slurry
P	external load (m)
m	material coordinate (m)
$D'(\vartheta)$	diffusivity in material coordinates (m^2/sec)
$K'(\vartheta)$	hydraulic conductivity in material coordinates (m/sec)
γ_c	particle specific gravity
M	initial material depth of slurry (m)
I	cumulate volume of filtrate (m)
$F(\Theta)$	flux–concentration relation
Θ	$(\vartheta - \vartheta_n)/(\vartheta_0 - \vartheta_n)$

Acknowledgments

Discussions with Drs. C. J. Barnes, J. R. Philip, and I. White of this Division are gratefully acknowledged.

REFERENCES

1. D. E. Smiles, *Chem. Eng. Sci.*, *25*, 985 (1970).
2. D. E. Smiles, *Ibid.*, *33*, 1355 (1978).
3. D. E. Smiles, *Aust. J. Soil Res.*, *14*, 389 (1976).
4. D. E. Smiles, *Sep. Sci.*, *11*, 1 (1976).
5. J. R. Philip, *Aust. J. Soil Res.*, *7*, 99 (1969).
6. J. R. Philip, *Soil Sci.*, *116*, 328 (1973).
7. J. R. Philip and J. H. Knight, *Ibid.*, *117*, 1 (1974).
8. D. E. Smiles and M. J. Rosenthal, *Aust. J. Soil Res.*, *6*, 237 (1968).
9. D. E. Smiles, *Soil Sci. Soc. Am. J.*, *42*, 11 (1978).
10. C. Matano, *Jpn. J. Phys.*, *8*, 109 (1933).
11. D. E. Smiles, *Soil Sci.*, *117*, 140 (1974).

Received by editor August 1, 1978